Supporting Information

Guney et al. 10.1073/pnas.1100072108

SI Materials and Methods

PCR and Genotyping. Genotyping of *CTGF*$^{e2COIN/e2COIN}$ mice was performed by PCR on DNA isolated from ear punches using the following primers: forward 5′ cac ttt cta ctc tgt gac 3′; and reverse 5′ cct tac atg ttt tac tag 3′. PCR amplification of the connective-tissue growth factor (CTGF) wild-type exon2 was used to distinguish *CTGF*$^{e2COIN/e2COIN}$ mice from *CTGF*$^{e2COIN/+}$ mice using the following primers: forward 5′ cct gct atg ggc cag gac tg 3′ and reverse 5′ cca aaa ggt gag gcc tct gc 3′. Inversion of the *CTGF*^{e2COIN} allele following Cre-mediated recombination was confirmed by PCR using DNA isolated from pancreatic tissue sections using the following primers: forward 5′ cct tac atg ttt tac tag 3′ and reverse 5′ ctc aga gta ttt tat cct cat ctc 3′.

Tissue Dissection, Preparation, and Histology. For embryonic studies, the morning of the vaginal plug was considered to be E0.5. Digestive organs were dissected in cold PBS and fixed immediately in 4% paraformaldehyde at 4 °C for 1 to 1.5 h. Tissues were dehydrated, embedded in paraffin, and sectioned at 5 μm. Serial sections were deparaffinized and rehydrated using a decreasing ethanol series to distilled water. Details for antibodies used in indirect protein localization can be found below.

Immunolabeling. Protein localization was assessed by incubation of tissue sections with the following primary antibodies: guinea pig anti-insulin (1:1,000; Upstate), rabbit anti-glucagon (1:1,000, Millipore), rabbit anti-Pdx-1 (1:1,000, from Christopher V. E. Wright, Vanderbilt University, Nashville, TN), rabbit anti-phosphorylated histone H3 (pH3, 1:200; Millipore), and mouse anti-Neurogenin3 (Ngn3, 1:1,000; Developmental Studies Hybridoma Bank, University of Iowa, Iowa City, IA), rat anti-platelet endothelial cell-adhesion molecule (anti-PECAM) (1:50; BD Pharmingen), mouse anti-Ki67 (1:500; BD Pharmingen), and rabbit anti-MafA (1:500; Bethyl Laboratories). Ducts were labeled with biotinylated *Dolichos biflorus* agglutinin (DBA, 1:1,000; Vector Laboratories) followed by detection with Cy3-conjugated streptavidin (1:500; Vector Laboratories). Detection of pH3 and Ngn3 required antigen retrieval in 10 mM sodium citrate buffer, pH 6.0. Slides were microwaved at full power until boiling and then boiled for 6 min. Ngn3 detection required tyramide signal amplification (Invitrogen). Ki67 and MafA staining required antigen retrieval in TEG buffer (pH 9.0) for 10 min at 40% power. PECAM staining was performed on paraffin sections using trypsin antigen retrieval, followed by an anti-rat biotinylated secondary antibody (1:500; Vector Laboratories) and TSA amplification. All primary antibodies were incubated overnight in a humid chamber at 4 °C. Primary antibodies were detected by species-specific donkey secondary antibodies conjugated to either Cy2 or Cy3 flurophores (1:200; Jackson ImmunoResearch Laboratories, Inc.). Flurophores were excited using an Olympus BX41 research microscope and digital images were captured using MagnaFire software (Optronics Engineering). TIFF images from each experiment were processed identically with Adobe Photoshop. X-gal staining was performed as previously described (1).

Proliferation of α and β Cells. Entire pancreata were serially sectioned and slides were immunolabeled for pH3 and insulin or glucagon. One section per slide was analyzed every 250 μm (7–10 sections per animal) throughout the pancreas. Every insulin- or glucagon-positive cell in that section was photographed and the total number of cells positive for insulin or glucagon was counted, as were the number of proliferating cells (colabeled for hormone and pH3) using Metamorph 6.1 software (Molecular Devices). The percentage of proliferating α or β cells was determined by dividing the number of proliferating cells by the total number of hormone-positive cells. For quantifying MafA$^+$ cell proliferation, double immunolabeling for MafA and Ki67 was used. The percentage of MafA$^+$ nuclei that were proliferating was determined by dividing the number of double-positive nuclei by the number of MafA$^+$ nuclei.

Insulin and Glucagon Area/Percentage Endocrine Area. Entire pancreata were serially sectioned and slides were immunolabeled for insulin and glucagon. One section was photographed every 250 μm throughout the pancreas. Using Metamorph 6.1 software, the insulin- and glucagon-positive area of each section was determined by thresholding. The percentage of the total endocrine area that was composed of insulin or glucagon was calculated. For the CTGF overexpression studies, the percentage of the pancreas area composed of endocrine tissue was calculated by combining the insulin- and glucagon-positive area on each section divided by the total pancreas area of each section.

Quantification of Ngn3-Positive Cells. Entire E14.5 pancreata were sectioned and slides were immunolabeled for Ngn3 and DAPI. One section every 150 μm was photographed (approximately six sections per embryo were analyzed). The number of Ngn3-positive nuclei were counted and divided by the total pancreatic epithelial area in micrometers squared.

Islet Microvascular Density. The proportion of the islet composed of blood vessels was determined by immunolabeling for insulin and PECAM. At least five pancreatic sections were analyzed and the PECAM-positive area of every islet (designated as containing 10 cells or more) per section was quantified using Metamorph. The total PECAM area was divided by the total insulin-positive area to determine the percentage of blood-vessel area.

Real-Time PCR. Pancreata were dissected and placed immediately into RNAlater (Ambion). Total RNA was extracted using the RNAqueous kit (Ambion) according to the manufacturer's instructions. RNA concentration and integrity were assessed using the ND-1000 Spectrophotometer (NanoDrop) and the 2100 Electrophoresis Biolanalyzer (Agilent) at the Vanderbilt Microarray Shared Resource. cDNA was synthesized using the SuperScript III First-Strand synthesis system (Invitrogen). Reactions were carried out in technical duplicate with iQ SYBR Green supermix (Bio-Rad) according to the manufacturer's instructions at an annealing temperature of 58 °C. Data were collected using an iCycler iQ Real-time PCR Detection System (Bio-Rad) and software (Bio-Rad). Primers were optimized by melting curve and standard curve assays first before application. Expression levels were normalized against the levels of hypoxanthineguanine phosphoribosytransferase (HPRT).

Real-Time PCR Primers. The following primers were used to detect total CTGF: forward 5′ ttc tgc gat ttc ggc tcc 3′ and reverse 5′ acc atc ttt ggc agt gca ca 3′. Primers used to detect endogenous CTGF were designed against the 3′UTR, which is absent from the CTGF cDNA: forward 5′ ctg ggg aca atg aca tct 3′ and reverse 5′gtt cgt gtc cct tac ttc ct 3′.

1. Crawford LA, et al. (2009) Connective tissue growth factor (CTGF) inactivation leads to defects in islet cell lineage allocation and beta-cell proliferation during embryogenesis. *Mol Endocrinol* 23:324–336.

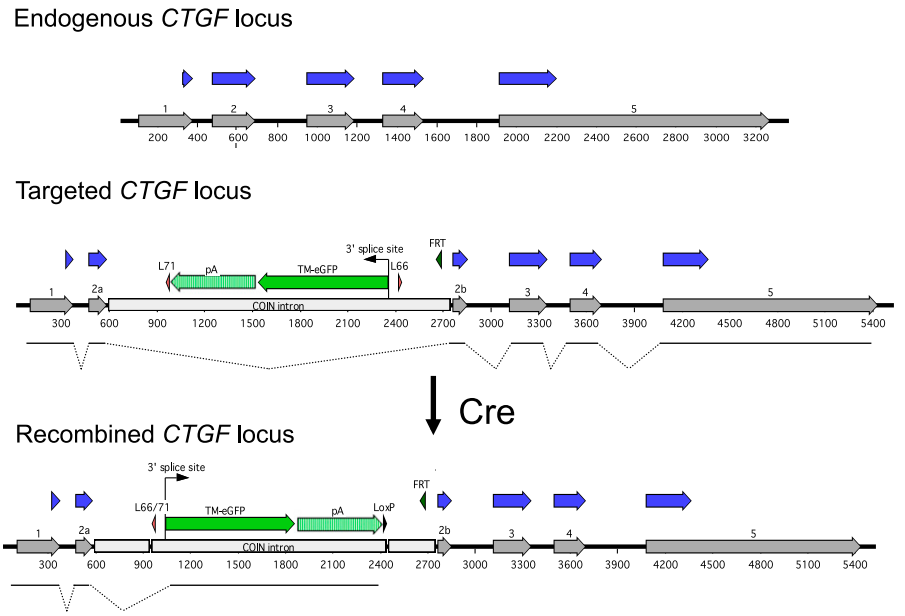

Fig. S1. Schematic of *CTGF* COIN allele used in these studies. (*Top*) the endogenous *CTGF* locus. Gray arrows indicate exons; blue arrows indicate coding regions. Using Velocigene technology (1) the COIN intron, containing a 3′ splice acceptor site, was introduced into exon 2 of *CTGF*, splitting it into two parts (*Middle*). In the absence of Cre recombinase, splicing around the COIN intron (line drawing below locus) results in a normal *CTGF* full-length message and protein being produced. In the presence of Cre (*Bottom*), the COIN intron is inverted introducing a novel splice acceptor site to which the 5′ half of exon 2 becomes fused producing a truncated *CTGF* message (line drawing below locus) that lacks the functional domains of the CTGF protein. This allele was first reported in Canalis et al. (2).

1. Valenzuela DM, et al. (2003) High-throughput engineering of the mouse genome coupled with high-resolution expression analysis. *Nat Biotechnol* 21(6):652–259.
2. Canalis E, Zanotti S, Beamer WG, Economides AN, Smerdel-Ramoya A (2010) Connective tissue growth factor is required for skeletal development and postnatal skeletal homeostasis in male mice. *Endocrinology* 151(8):3490–3501.

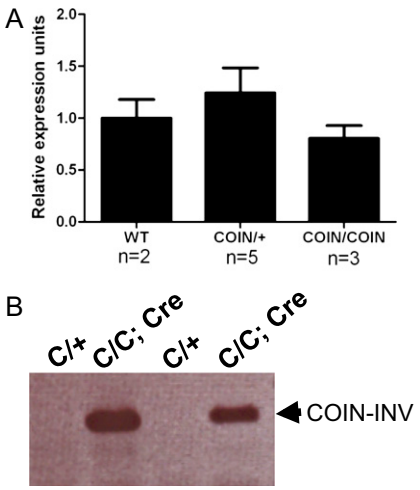

Fig. S2. (*A*) Quantification of real-time PCR for *CTGF* expression in wild type (WT), $CTGF^{e2COIN/+}$ (COIN/+), and $CTGF^{e2COIN/e2COIN}$ (COIN/COIN) pancreata at E18.5. (*B*) PCR to specifically detect the inverted form of the $CTGF^{e2COIN}$ allele (COIN-INV) using DNA isolated from pancreatic sections from $CTGF^{e2COIN/+}$ (C/+) and $CTGF^{e2COIN/e2COIN}$;*Pdx-1*-Cre (C/C;Cre) pancreata.

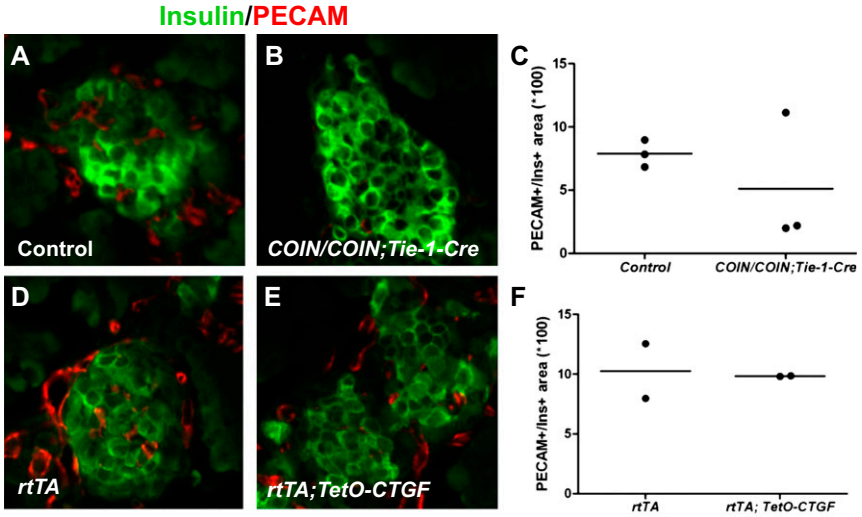

Fig. S3. Islet vascular density in *CTGF* mutant and over-expressing pancreata. (*A*) Control and (*B*) $CTGF^{COIN/COIN}$;*Tie-1-Cre* E18.5 pancreata, and (*D*) Control *rtTA* and (*E*) *RIP-rtTA;TetO-CTGF* P1 pancreata were immunolabeled for insulin (green) and PECAM (red). (*C* and *F*) Quantification of the ratio of PECAM area to insulin-positive area for the *Tie-1-Cre* mutants and CTGF-overexpressing animals, respectively. The line represents the average for each group. Magnification, 400×.

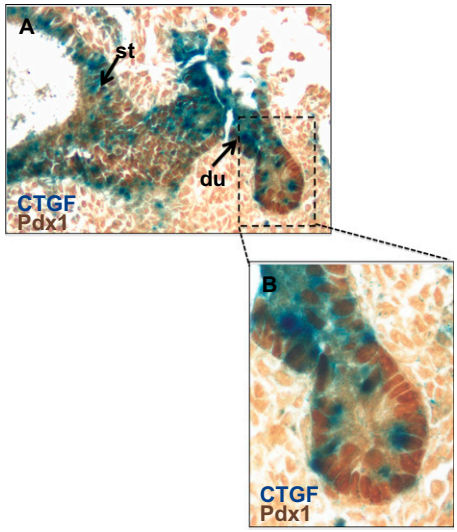

Fig. S4. *CTGF* is expressed in the early pancreatic bud epithelium. $CTGF^{lacZ/+}$ E10.5 embryos were stained with X-gal in whole mount to assay for *CTGF* expression (blue). Sections were immunolabeled with antibodies against Pdx1 to determine the location of the posterior foregut endoderm at this stage, and in particular the emerging pancreatic buds (boxed area magnified in *B*). (*A*) Pdx1 protein (brown) was detected in the endodermal epithelium of the posterior stomach, duodenum and pancreas, as expected. At this stage, *CTGF* expression was observed throughout the $Pdx1^+$ domain, but only in scattered cells within the pancreatic epithelium. *CTGF* was not expressed to any great extent in the surrounding pancreatic mesenchyme at this stage. St: stomach; du: duodenum. Magnification in *A*, 200×.

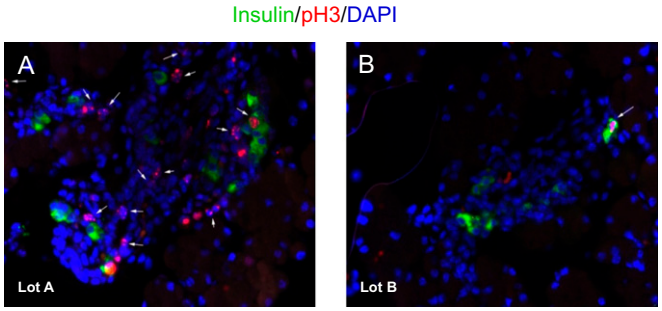

Fig. S5. Sensitivity of the pH3 antibody to detect proliferating cells varied depending on the antibody lot. Representative images of adjacent slides from pancreata that were stained with two different lots of pH3 antibody. (*A*) Lot A was used to stain sections of control and *CTGF*$^{e2COIN/e2COIN}$*;Tie-1-Cre* pancreata and (*B*) lot B was used to stain control and *CTGF*$^{e2COIN/e2COIN}$*;Pdx-1-Cre* and *CTGF*$^{e2COIN/e2COIN}$*;Ngn-3-Cre* pancreata. Arrows indicate proliferating cells. (Magnification: 400×.)

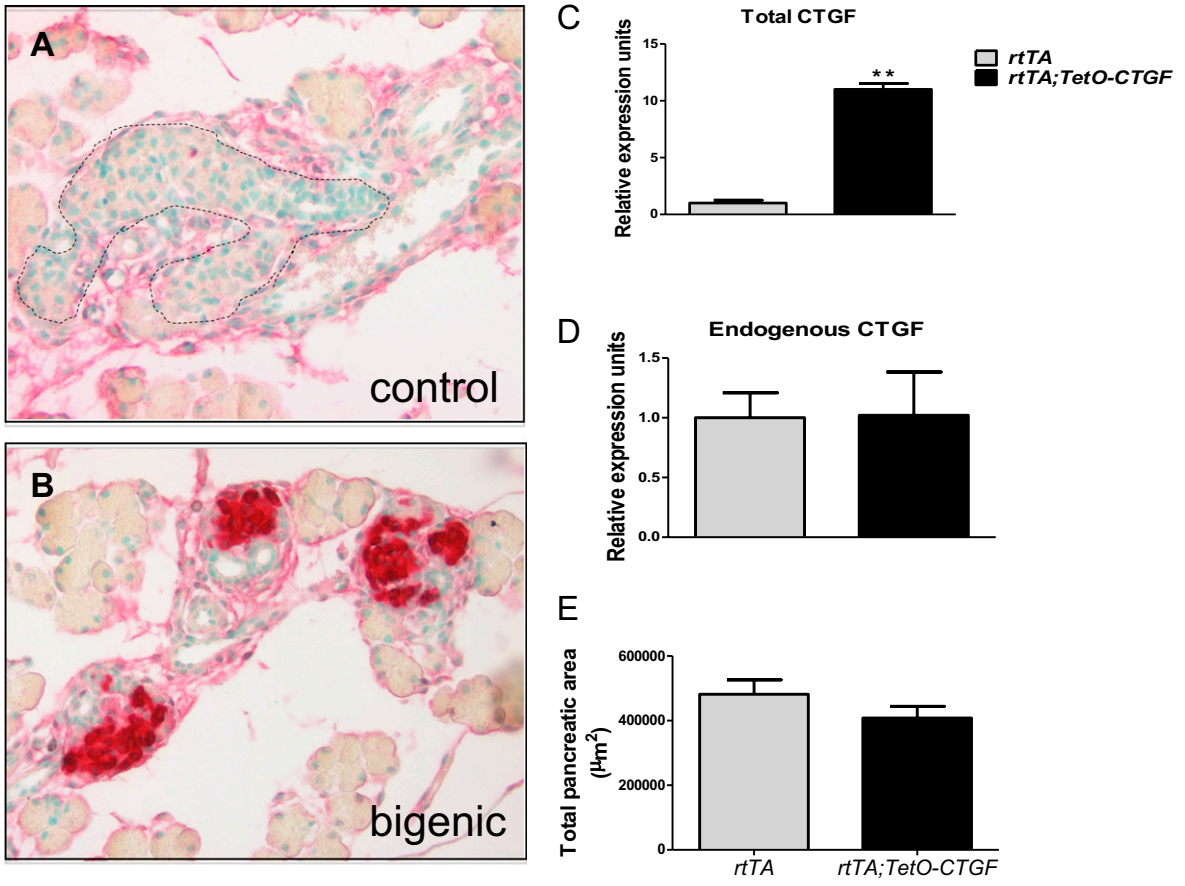

Fig. S6. (*A* and *B*) CTGF protein (red) was clearly elevated in islets from P1 bigenic pancreata compared with controls following doxycycline (DOX) treatment (magnification, 200×). DOX treatment was initiated at E9.5 in pregnant mothers' drinking water. Nuclei are blue. (*C*) *Ctgf* expression in bigenic pancreata (black bars) was increased ~10-fold compared with control embryos (gray bars) at E16.5. (*D*) Primers specifically amplifying endogenous *Ctgf* demonstrated that endogenous *Ctgf* levels are not significantly different between control and CTGF overexpressing embryos. (*E*) Total pancreatic area was not significantly changed between control (*rtTA*) and bigenic (*rtTA;TetO-CTGF*) neonates at P1, nor did we observe increased fibrosis in CTGF overexpressing pancreata. $^{**}P < 0.0001$. $n = 3$ for all groups.

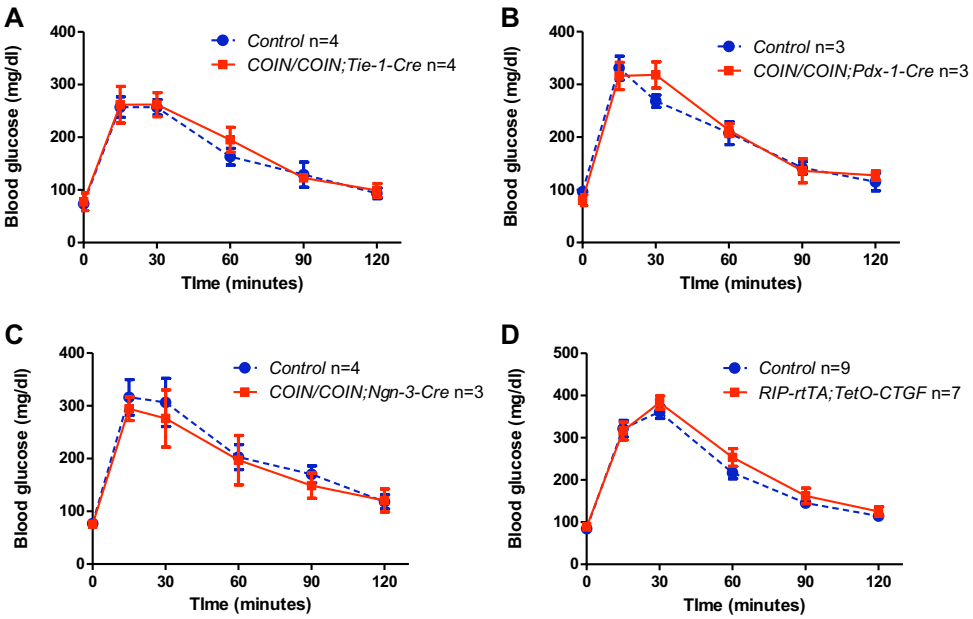

Fig. S7. Intraperitoneal glucose tolerance tests were performed between 2 and 4 mo of age on *CTGF* mutant animals (*A*–*C*) and animals in which CTGF was overexpressed during embryogenesis (*D*). There was no difference noted in any group.